Published in final edited form as:
J Neurochem. 2010 December ; 115(6): 1350–1362. doi:10.1111/j.1471-4159.2010.07035.x.

NR2B-NMDA receptor mediated modulation of the tyrosine phosphatase STEP regulates glutamate induced neuronal cell death

Ranjana Poddar[*], **Ishani Deb**[*], **Saibal Mukherjee**, and **Surojit Paul**[¶]
University of New Mexico Health Sciences Center, *Department of Neurology, 1 University of New Mexico, Albuquerque, NM – 87131

Abstract

The present study examines the role of a neuron-specific tyrosine phosphatase (STEP) in excitotoxic cell death. Our findings demonstrate that p38 MAPK, a stress-activated kinase that is known to play a role in the etiology of excitotoxic cell death is a substrate of STEP. Glutamate-mediated NMDA receptor stimulation leads to rapid but transient activation of p38 MAPK, which is primarily dependent on NR2A-NMDA receptor activation. Conversely, activation of NR2B-NMDA receptors leads to dephosphorylation and subsequent activation of STEP, which in turn leads to inactivation of p38 MAPK. Thus during transient NMDA receptor stimulation, increases in STEP activity appears to limit the duration of activation of p38 MAPK and improves neuronal survival. However, if NR2B-NMDA receptor stimulation is sustained, protective effects of STEP activation are lost, as these stimuli cause significant degradation of active STEP, leading to secondary activation of p38 MAP kinase. Consistent with this observation, a cell transducible TAT-STEP peptide that constitutively binds to p38 MAPK attenuated neuronal cell death caused by sustained NMDA receptor stimulation. The findings imply that the activation and levels of STEP are dependent on the duration and magnitude of NR2B-NMDA receptor stimulation and STEP serves as a modulator of NMDA receptor dependent neuronal injury, through its regulation of p38 MAPK.

Keywords

p38 MAPK; STEP; glutamate; NR2A; NR2B; tyrosine phosphatase

INTRODUCTION

Excitotoxic glutamate receptor activation is implicated in neuro-degeneration following ischemic insults, post-traumatic lesions and a range of other neurological disorders (Lipton and Rosenberg 1994; Arundine and Tymianski 2004). In pathological conditions excessive release of the neurotransmitter glutamate leads to sustained activation of NMDA-type glutamate receptors and a deleterious cascade of intracellular events that include Ca^{2+} overload and activation of effectors such as p38 mitogen activated protein kinase (p38 MAPK). Recent findings suggest the existence of two functionally distinct pools of NMDA receptors defined by the presence of NR2A (NR2A-NMDAR) or NR2B (NR2B-NMDAR) containing subunits (Luo et al. 1997; Tovar and Westbrook 1999; Kohr 2006). NR2B-

[¶]Corresponding Author: Surojit Paul, PhD, University of New Mexico Health Sciences Center, Department of Neurology, 1, University of New Mexico, Albuquerque, NM – 87131, Tel: (505) 272-0610, Fax: (505) 272-8306, spaul@salud.unm.edu.
[*]These two authors have contributed equally to this work.

NMDARs are generally thought to be involved in triggering cell death and subsequent brain damage following an excitotoxic insult (Liu et al. 2007; Tu et al. 2010). However pharmaceutical application of NR2B-NMDAR antagonists have been unsuccessful in clinical trials, since they interfere with physiological functions of these receptors, in addition to blocking excitotoxic cascades (Rodrigues et al. 2001; Zhao et al. 2005; Walker and Davis 2008). An alternative approach that may improve treatment of excitotoxic insults involves targeting of components of intracellular signaling cascades downstream of NMDA receptor signaling.

The p38 MAPK pathway has been shown to be involved in mediating the pathogenesis of glutamate excitotoxicity (Barone et al. 2001a; Barone et al. 2001b). While the role of NMDA receptors in the activation of p38 MAPK is well established (Mukherjee et al. 1999; Waxman and Lynch 2005), the precise intracellular mechanisms that regulate the duration and magnitude of p38 MAPK are not clearly understood. A goal of the present work was to determine whether the p38 MAPK activation is significantly regulated by the neuron-specific tyrosine phosphatase, STEP (striatal-enriched tyrosine phosphatase) and whether this could be targeted to limit excitotoxic injury.

STEP, also known as PTPN5, is expressed specifically in neurons of the striatum, neo-cortex and hippocampus (Boulanger et al. 1995). $STEP_{61}$ and $STEP_{46}$, the two STEP isoforms (Bult et al. 1997) contain a highly conserved substrate-binding domain termed as the kinase interacting motif or KIM domain (Pulido et al. 1998). Phosphorylation of a critical serine residue within the KIM domain is mediated through dopamine/D1 receptor dependent activation of the Protein Kinase A (PKA) pathway (Paul et al. 2000). Dephosphorylation of this residue by Ca^{2+} dependent phosphatase calcineurin, following glutamate/NMDA receptor stimulation, renders STEP active in terms of its ability to bind to its substrates (Paul et al. 2003). Active STEP can bind to and inhibit the activity of ERK (extracellular regulated kinase 1/2) MAP kinase (Paul et al. 2007).

The aim of the present study was to investigate the functional significance of STEP's activation following excitotoxic NMDAR stimulation. Our findings show that NR2B-NMDAR stimulation leads to activation of STEP. Active STEP can contribute to neuronal cell survival by down regulating p38 MAPK activity. However sustained NR2B-NMDAR stimulation results in the degradation of active STEP, and relieves its inhibitory effect on p38 MAPK and results in cell death.

MATERIALS AND METHODS

Materials and reagents

Pregnant female and adult (250 gm) Sprague-Dawley rats were from Harlan Laboratories (Livermore, CA). Antibodies used were as follows: polyclonal anti-p38, rabbit monoclonal anti-phospho-p38 ($T^{P}EY^{P}$ and TEY^{P}) from Cell Signaling (Danvers, MA), monoclonal anti-myc from Santa Cruz Biotechnology (Santa Cruz, CA), monoclonal anti-Flag and polyclonal anti-tubulin from Sigma-Aldrich (St. Louis, MO), polyclonal anti-MAP2 from Chemicon, monoclonal anti-V5 and anti-V5-HRP from Invitrogen, monoclonal anti-STEP from Novus Biologicals (Littleton, CO). All secondary antibodies were from Cell Signaling. All tissue culture reagents were obtained from Invitrogen (Carlsbad, CA). All other reagents were from Sigma-Aldrich. Approval for animal experiments was given by the University of New Mexico, Health Sciences Center, Institutional Animal Care and Use Committee.

Plasmids and Transfection

$STEP_{46}$ cDNA was constructed in mammalian expression vector pcDNA 3.1 encoding a C-terminal V5 and His tag (Invitrogen). Point mutants were generated by PCR-based site-

directed mutagenesis using Pfu Turbo DNA polymerase (Stratagene, La Jolla, CA) according to the manufacturer's protocol. All mutations were verified by nucleotide sequencing. The p38α, β and γ cDNAs with a FLAG tag at the C-terminal were gifts from Dr. Anton Bennett, Yale University.

In vitro phosphorylation of STEP and tyrosine phosphatase assay

GST, GST-$STEP_{46}$ and GST-$STEP_{46}$ C300S fusion proteins were generated as described previously (Paul et al. 2000). For *in vitro* binding studies GST fusion proteins were incubated with p38α MAPK recombinant protein (EMD Biosciences, CA) overnight at 4°C in a buffer containing 50 mM Tris-HCl, pH 7.0, 100 mM NaCl, 5 mM dithiothreitol, 0.01% Brij 35 and 2 mM EDTA. Samples were then incubated with Glutathione-sepharose beads (2 hr) and washed extensively. Bound proteins were eluted using SDS-sample buffer and processed for immunoblot analysis. *In vitro* phosphorylation of GST-$STEP_{46}$ fusion protein by PKA was done as described earlier (Paul et al. 2003). Phosphorylated and non-phosphorylated STEP was incubated with active p38α MAPK recombinant protein for specified time periods (0, 5, 7.5 and 10 min). The reactions were stopped by addition of SDS-sample buffer and the samples were processed for immunoblot analysis.

Affinity Column Chromatography

$STEP_{46}$ C300S cDNA, a substrate-trapping variant of $STEP_{46}$, was cloned into the E. Coli expression vector pET104.1, with a six-histidine tag at the C-terminal (Invitrogen). The vector provides a biotin conjugation site at the N-terminus of the protein to allow *in vivo* biotinylation of the over-expressed protein by endogenous E. Coli biotin ligases. The purified biotinylated protein was coupled to streptavidin agarose beads (Thermo Scientific, Rockford, IL, USA). Using striatal homogenates from rat brain substrate-trapping experiments were performed as described before (Nguyen et al. 2002). Bound proteins were eluted with 0.1 M glycine, pH 2.8 and processed for immunoblot analysis.

Purification of TAT-STEP-myc fusion protein

$STEP_{46}$ ΔPTP cDNA ($STEP_{46}$ 1–107) that lacks the C-terminal phosphatase domain was sub-cloned in a pTrc-His-myc-TOPO expression vector (Invitrogen). To render the peptide cell permeable an 11 amino acid peptide called TAT was inserted at the N-terminal of the $STEP_{46}$ ΔPTP cDNA (Paul et al. 2007). A point mutation was introduced at the serine residue within the KIM domain (S49A) by site-directed mutagenesis. $STEP_{46}$ ΔPTP was expressed in E. Coli and the fusion protein was purified using BD-Talon resin (BD Biosciences, Bedford, MA, USA).

Cell culture and stimulation

Primary neuronal cultures were obtained from 16–17 day old rat embryos as described previously (Paul et al. 2003). Briefly, the striatum and the adjoining cortex was dissected, the tissue dissociated mechanically and resuspended in DMEM/F-12 (1:1)-containing 5% fetal calf serum (FCS). Cells (6×10^6 cells/dish) were plated on poly-D-lysine-coated tissue culture dishes (BD Biosciences) and grown for 12–14 days at 37°C in a humidified atmosphere (95:5% air:CO_2 mixture). For receptor stimulation cells were treated with glutamate or NMDA for the indicated times and then processed for immunoprecipitation or immunoblot analysis as described earlier (Paul et al. 2003). Glycine concentration in the medium during glutamate treatment was 1 μM. In some experiments APV or CNQX were added 5 min after the addition of glutamate; ifenprodil and Ro 25-6981 were added 10 min before addition of glutamate. Some cultures were treated with the TAT-STEP-myc peptide (4 μM) or SB-203580 (2.6 μM) prior to or along with glutamate treatment. Densitometric analysis of immunoblots was performed using Image J software (NIH, Bethesda, MD,

USA). Statistical comparison was carried out using one-way analysis of variance (ANOVA, Bonferroni's multiple comparison test) and differences were considered significant when $p < 0.05$.

Immunocytochemistry and Hoechst DNA staining

Hela cells transfected with $STEP_{46}$ cDNA or neuron cultures grown for 12–14 days were processed for immunocytochemistry as described earlier (Paul et al. 2003). Hela cells were immunostained with anti-phospho-p38 (T^PEY^P, 1:100) and/or anti-STEP (1:250) antibodies. Neuronal cells were immunostained with ant-myc (1:100), anti-MAP2 (1:250) or anti-phospho p38 (T^PEY^P, 1:100) antibodies. Alexa Fluor 488 conjugated anti-mouse IgG or Cy3 conjugated anti-rabbit IgG were used as secondary antiboies (1:250 each). In some cases neurons were subjected to staining with Hoechst 33342 dye for 15 minutes to assess nuclear damage. Imaging was performed with a Zeiss Axiovert 200M fluorescence microscope with attached AxioCam CCD camera using 20X objective lens. To quantitatively assess the percentage of pyknotic nuclei a total of 1000 cells were counted for each set of experiments. Mean ± s.e.m. (n = 3) were used for statistical comparison using ANOVA (Bonferroni's multiple comparison test). Differences were considered significant when $p < 0.05$.

Stereotactic surgery and Immunohistochemistry

For intra-striatal injection of glutamate adult male rats were anesthetized with 2% isoflurane in 70% nitrous oxide and 30% oxygen. A burr hole was drilled and a micropipette was lowered into the right striatum using the following coordinates (Paxinos and Watson 1986): 5.0 mm lateral to bregma and 5.5 mm ventral to the skull surface. 1 μl of TAT-STEP-myc peptide or PBS was infused into the right striatum over a time period of 2 min. The injector was left in place for an additional 2 min to minimize back-flux of the solution. After injector withdrawal, the wound was sutured and the rats returned to their cages. In some animals 30 nmol of glutamate in 1 μl PBS or PBS alone (control) was infused into the striatum 30 min after infusion of TAT-STEP-myc peptide or PBS. At the specifies time points after infusion rats were anesthetized, perfused intracardially with 4% paraformaldehyde and processed for cryosectioning followed by immunohistochemistry with anti-myc antibody (1:100) (Paul et al. 2007). Sections were then treated with Hoechst 33342 dye for DNA stain, mounted using vectashield and analyzed using fluorescent microscopy. For assessment of nuclear damage, the percentage of pyknotic nuclei was estimated in five different fields within the striatum of each section immediately below the site of needle injection. For sections obtained from TAT-STEP-myc peptide injected animals the percentage of cells positively stained with anti myc-antibody within the same fields were also determined. Each experiment was repeated at least 3 times. Statistical comparison was carried out using ANOVA (Bonferroni's multiple comparison test) and differences were considered significant when $p < 0.05$.

RESULTS

Glutamate-NMDA receptor mediated regulation of p38 MAPK in neurons

We first determined the temporal profile of p38 MAPK phosphorylation following an excitotoxic insult. Neuronal cultures (12–14 days *in vitro*) were treated with 100 μM glutamate for varying times and cell lysates were analyzed by immunoblotting with a phospho-specific antibody that recognizes p38 only when phosphorylated at both the regulatory threonine and tyrosine residues (T^PEY^P-p38). Our results show a transient increase in phosphorylation of p38 MAPK within 2–5 min of glutamate stimulation. This was followed by a time-dependent decrease in p38 phosphorylation, which returned to near basal levels by 30 min (Fig. 1A). Total p38 MAPK level remained unaltered by this treatment. Treatment with 100 μM NMDA caused a similar transient activation of p38

MAPK (Fig. 1B) as was seen with glutamate suggesting that NMDAR activation was required for phosphorylation of p38 MAPK.

To explore the contribution of NMDARs in the dephosphorylation of p38 MAPK, a selective NMDA receptor antagonist (APV, 200 μM), was applied 5 min after incubation with glutamate. The delayed treatment with APV inhibited the glutamate-induced dephosphorylation of p38 MAPK (Fig. 1C). However a similar treatment with CNQX (20 μM), a non-NMDA receptor antagonist failed to prevent the glutamate-induced dephosphorylation of p38 MAPK (Fig. 1D). These observations in conjunction with previous studies (Waxman and Lynch 2005) suggest that both phosphorylation and dephosphorylation of p38 MAPK in neurons require NMDA receptor activation.

We next examined the roles of NR2A- and NR2B-NMDARs in the dephosphorylation of p38 MAPK. Neurons were treated with 100 μM glutamate in the presence or absence of selective NR2B-NMDAR antagonists, ifenprodil and Ro 25-6981. As shown in Figures 1E and F these antagonists had no effect on the initial phosphorylation of p38 MAPK by 5 min, however, the subsequent dephosphorylation of p38 MAPK (measured at 30 min) was significantly reduced, suggesting that NR2B-NMDAR stimulation are required for the dephosphorylation of p38 MAPK.

NR2B-NMDAR mediated activation of STEP followed by its proteolytic cleavage

A potential candidate that might mediate the NR2B-NMDAR dependent dephosphorylation of p38 MAPK is the tyrosine phosphatase STEP. Under basal condition STEP is phosphorylated at the PKA site in the KIM domain (Ser221 in $STEP_{61}$ and Ser49 in $STEP_{46}$) (Paul et al. 2000). Stimulation of NMDARs by glutamate leads to time-dependent dephosphorylation and activation of STEP, which begins at 5 min and leads to complete dephosphorylation by 30 min. Using a phospho-specific antibody (against the PKA site) it has also been shown that dephosphorylation of STEP results in downward shift in mobility of the STEP band (Paul et al. 2003). Consistent with these earlier findings incubation of neurons with glutamate resulted in a marked decrease in the upper band and the appearance of a predominant lower band, indicating that $STEP_{61}$ is rapidly dephosphorylated following glutamate treatment (Fig. 2A & B, lane 2). Pre-incubation with either Ro 25-6981 or ifenprodil blocked the downward shift in the mobility of the upper band, supporting a role for NR2B-NMDAR in the dephosphorylation of $STEP_{61}$ (Fig. 2A & B, lane 3).

We also examined the temporal profile of STEP's activation following treatment with glutamate (100 μM, 30 min), by immunoblot analysis with anti-STEP antibody. Figure 2C shows that 30 minute after termination of glutamate treatment STEP was subjected to proteolytic cleavage resulting in the appearance of a cleaved product of ~33 kDa ($STEP_{33}$), which increased over time (~5 fold 1 hr). Analyzing the same samples with anti-$T^{P}EY^{P}$ antibody showed an increase in phosphorylation of p38 MAPK 0.5 – 1 hr after termination of glutamate exposure (Fig. 2D). To determine the involvement of NR2B-NMDAR in the cleavage of STEP neurons were incubated with Ro 25-6981 prior to treatment with glutamate (100 μM glutamate, 30 min). Pre-incubation with Ro 25-6981 blocked the dephosphorylation as well as the proteolytic cleavage of $STEP_{61}$ (Fig. 2E). These results imply that glutamate-mediated NR2B-NMDAR stimulation leads to initial activation of STEP, and then a progressive decrease in STEP levels over time in the post-glutamate period. When taken together with results above (Fig. 1), these observations raise the possibility that active STEP may play an initial role in dephosphorylation of p38 MAPK and may serve as a key regulator of p38 MAPK activation in excitotoxicity. However degradation of STEP may lead to the secondary activation of p38 MAPK.

p38 MAPK is a substrate of STEP

To determine whether p38 MAPK is a potential substrate of STEP, striatal homogenates from rat brain were subjected to affinity purification with a substrate-trapping mutant of STEP ($STEP_{46}$ C300S). Immunoblot analysis of the eluant showed that p38 MAPK was part of the protein complex bound to STEP (Fig. 3A). To determine if STEP can directly interact with p38 MAPK, purified GST-$STEP_{46}$ or GST-$STEP_{46}$ C300S protein coupled to glutathione sepharose beads was incubated with a p38 MAPK fusion protein. Immunoblot analysis revealed that both variants of STEP were able to pull down p38 MAPK (Fig. 3B). To test the ability of active STEP to dephosphorylate p38 MAPK *in vitro*, purified GST-$STEP_{46}$ was incubated with phosphorylated p38 MAPK fusion protein (active form) for varying time periods. Immunoblot analysis with an antibody that recognizes p38 only when phosphorylated at the tyrosine residue (TEY^P p38) revealed a time-dependent decrease in tyrosine phosphorylation of p38 MAPK (Fig. 3C, upper panel). The ability of phosphorylated STEP (phosphorylated at the PKA site in the KIM domain) to dephosphorylate active p38 MAPK was also measured. The data shows that phosphorylated STEP fails to dephosphorylate p38 MAPK (Fig. 3C, lower panel). These results suggest that p38 MAPK is a substrate of STEP and phosphorylation of STEP at the serine residue in the KIM domain inhibits the interaction between STEP and p38 MAPK.

To further clarify the mechanism by which STEP regulates p38 MAPK in intact cells V5-$STEP_{46}$ WT or one of its mutants that cannot be phosphorylated endogenously at the KIM domain site (S49A or S49A/C300S) were transfected in Hela cells. Immunoprecipitation of STEP using anti-V5 antibody followed by immunoblot analysis using anti-p38 antibody showed that both V5-$STEP_{46}$ S49A (dephosphorylated form of STEP) and V5-$STEP_{46}$ S49A/C300S (dephosphorylated and catalytically inactive mutant) were able to pull down endogenous p38 MAPK (Fig. 3D). In contrast the phosphorylated form (V5-$STEP_{46}$ WT) failed to bind to p38 MAPK. This suggests that in intact cells only the dephosphorylated form of STEP can interact with p38 MAPK.

The family of p38 MAPKs includes p38α, β, γ and δ isoforms, although only p38α and β, are expressed in the brain (Kumar et al. 2003). To determine whether STEP can interact with all four isoforms, Hela cells were co-transfected with V5-$STEP_{46}$ S49A and either p38α, β, γ and δ cDNA. Only p38α and β immunoprecipitated with STEP (Fig. 3E) suggesting a role of STEP in regulating the physiological function of these two isoforms in neurons.

Activation and subsequent nuclear translocation of p38 MAPK has been implicated in glutamate-NMDA receptor induced neuronal cell death (Waxman and Lynch 2005). To examine the role of STEP in regulating the nuclear translocation of active p38 MAPK, Hela cells were transfected with V5-$STEP_{46}$ WT or the S49A mutant and then treated with sorbitol. Consistent with earlier studies (Ingram et al. 2000) hyper-osmotic stress generated with sorbitol resulted in phosphorylation and subsequent nuclear translocation of active p38 MAPK (Fig. 3F). In the presence of V5-$STEP_{46}$ WT, sorbitol-mediated nuclear translocation of p38 MAPK was not affected. In contrast, expression of V5-$STEP_{46}$ S49A abolished nuclear translocation of active p38 MAPK (Fig. 3G). These results establish that only the dephosphorylated and active form of STEP can block phosphorylation and nuclear translocation of p38 MAPK.

The above findings show that p38 MAPK is inhibited by STEP and STEP's activation following glutamate/NMDA receptor stimulation correlates strongly with the inactivation of p38 MAPK. While these results suggest a neuroprotective role for active STEP, it is clear that under most excitotoxicity paradigms STEP activation is not sufficient to prevent neuronal injury. This is illustrated in Figure S1, where delayed neuronal death is observed following exposure of neuron cultures to 100 μM glutamate for 30 min, as has been

described in many prior reports (Kawasaki et al. 1997; Barone et al. 2001a). This delayed neuronal cell death was blocked by pre-incubation with SB-203580 a selective inhibitor of p38 MAPK. This confirms a central role of p38 MAPK in the excitotoxic cascade and emphasizes that any inhibitory effects of STEP were not sufficient to block p38 MAPK activation (Fig. S1). This is possibly due to the fact that sustained stimulation of NMDARs led to proteolytic cleavage of active STEP resulting in secondary activation of p38 MAPK.

TAT-STEP attenuates glutamate/NMDA receptor induced neuronal cell death

To directly test the hypothesis that interaction of STEP with p38 MAPK regulates neuronal injury we generated a cell permeable TAT-STEP-myc peptide (TAT-$STEP_{46}$ S49A ΔPTP-myc, see "Materials & Methods") that can constitutively bind to p38 MAPK. We first determined the temporal profile of intracellular uptake of the TAT-STEP-myc peptide. Neuronal cultures were incubated with the TAT-STEP-myc peptide for varying time periods (0, 5, 15, 30 or 120 min). Immunocytochemical analysis with anti-myc antibody showed that the peptide was detectable 15 min after application that peaked at 30 min and was present for the rest of the time studied (Fig. 4A). We then determined whether the TAT-STEP-myc peptide could bind to endogenous p38 MAPK. Neuronal cultures were incubated with the peptide for 30 min followed by immunoprecipitation with anti-myc antibody. Immunoblotting with anti-p38 antibody showed that the TAT-STEP-myc peptide forms a stable complex with p38 MAPK (Fig. 4B). We next examined whether pre-incubation with TAT-STEP-myc peptide or its co-application along with glutamate can block the initial phosphorylation and nuclear translocation of p38 MAPK at 5 min. Stimulation with glutamate (100 μM, 5 min) alone led to phosphorylation (Fig. 4C and D, upper panel, lane 2) and nuclear translocation of p38 MAPK (Fig. 4E, upper panel). Pre-incubation of neurons with TAT-STEP-myc peptide (30 min) prior to glutamate treatment blocked the phosphorylation (Fig. 4C, upper panel, lane 3) and nuclear translocation of p38 MAPK at 5 min (Fig. 4E, middle row). When the peptide was co-administered along with glutamate, it failed to block the initial phosphorylation (Fig. 4D, upper panel, lane 3) and nuclear translocation (Fig. 4E, lower panel) of p38 MAPK by 5 min. Finally, we examined if co-application of TAT-STEP-myc peptide along with glutamate can block the delayed phosphorylation and nuclear translocation of p38 MAPK at the post-glutamate period, between 0.5 – 1 hr. Neurons were incubated with glutamate (100 μM) for 30 min in the presence or absence of TAT-STEP-myc peptide and then processed for immunoblotting and immunocytochemical analysis 30 min after termination of glutamate treatment. Stimulation with glutamate alone led to phosphorylation (Fig. 4F, upper panel, lane 2) and nuclear translocation of p38 MAPK (Fig. 4G, upper row). Co-application of TAT-STEP-myc peptide blocked the phosphorylation (Fig. 4F, upper panel, lane 3) and nuclear translocation (Fig. 4G, lower row) of p38 MAPK.

We then evaluated the role of the initial p38 MAPK activation by 5 min as well as the delayed p38 MAPK activation between 0.5 – 1 hr (post-glutamate period) in neuronal injury following exposure to an excitotoxic dose of glutamate (100 μM, 30 min). For these experiments the TAT-STEP-myc peptide was applied to neuronal cultures either 30 min prior to glutamate treatment (100 μM, 30 min) or co-applied along with glutamate (100 μM, 30 min). 20 hr later cells were processed for Hoechst DNA staining and MAP2 staining to test for cell viability. The representative photomicrographs and the corresponding mean data (Fig. 5A & B) demonstrate that 16 ± 5% of the cells were apoptotic under basal conditions (no treatment). Following glutamate treatment 79 ± 7% of the cells became apoptotic. Pre-incubation with TAT-myc peptide (30 min) alone failed to attenuate glutamate induced neuronal cell death. Pre-incubation with TAT-STEP-myc peptide (30 min) prior to glutamate treatment greatly reduced the number of apoptotic cells to 26 ± 4%. Co-application of the TAT-STEP-myc peptide along with glutamate also reduced the number of

apoptotic cells to 30 ± 4%. This latter result is important when taken together with the results of the p38 MAPK activation above (Fig. 4). Thus TAT-STEP-myc peptide when co-administered along with glutamate failed to block the initial p38 MAPK activation by 5 min but still abolished the delayed p38 MAPK activation and greatly reduced neuronal injury. This is consistent with our hypothesis that neuronal injury following exposure to an excitotoxic dose of glutamate is primarily due to delayed activation of p38 MAPK following the proteolytic cleavage of STEP.

TAT-STEP-myc attenuates cell death in vivo

We next investigated whether the TAT-STEP-myc peptide infused in the brain can prevent excitotoxic injury *in vivo*. This was tested in the well-established model of glutamate microinjection into the striatum and evaluation of neuronal injury 24 hr later (Iadecola et al. 2001; Haelewyn et al. 2008). In initial experiments, uptake of the TAT-STEP-myc peptide into striatal cells was confirmed following stereotactic injection into the right striatum (Fig. 6A and B). Coronal brain sections of the striatum taken at different time points (12 and 24 hr) after infusion were examined immunohistochemically with anti-myc antibody. While no myc staining was observed in the contralateral striatum (left striatum), myc positive cells were detectable in the ipsilateral striatum (right striatum) infused with TAT-STEP-myc, at both the time points studied (Fig. 6C). In subsequent experiments animals were stereotactically injected with glutamate (30 nmol) in the presence or absence of TAT-STEP-myc peptide. 24 hr later coronal brain sections of the striatum were processed for immunohistochemical staining with anti-myc antibody and Hoechst DNA staining. The representative photomicrograph and the corresponding mean data (Fig. 6D) show a significant reduction in cell death in the presence of the peptide. Quantitative analysis further showed that 93 ± 1.1% of the cells that were transduced with TAT-STEP-myc peptide was protected against glutamate-induced cell death.

DISCUSSION

A key finding of the present study is that NR2B-NMDARs play a critical role in neuronal survival through activation of the tyrosine phosphatase STEP that in turn can limit the duration of activation of p38 MAPK. However, active STEP is susceptible to degradation on prolonged exposure to an excitotoxic insult leading to secondary activation of p38 MAPK. The ability of TAT-STEP-myc peptide to inhibit the delayed activation of p38 MAPK and attenuate cell death further suggests that activation of pro-apoptotic pathways are possibly downstream of the secondary p38 MAPK activation. It is also conceivable that in addition to p38 MAPK there may be other potential substrates that STEP could act upon to confer neuroprotection.

This study in conjunction with previous findings (Waxman and Lynch 2005) indicates that stimulation of NR2A-NMDARs leads to a rapid but transient activation of p38 MAPK. Previous studies have also shown that glutamate-mediated NR2A-NMDAR stimulation leads to transient activation of ERK MAPK (Kim et al. 2005). Such transient activation of ERK and p38 MAPK pathways under physiological conditions is thought to be involved in the induction of long-term potentiation and long-term depression respectively (Bolshakov et al. 2000; Zhu et al. 2002; Gisabella et al. 2003; Thomas and Huganir 2004; Wang et al. 2004), two opposing forms of synaptic plasticity that are thought to contribute to learning and memory. The transient nature of p38 and ERK activation following NR2A-NMDAR stimulation suggests sequential activation of a stimulatory and an inhibitory pathway. The inhibitory pathway involves the tyrosine phosphatase STEP. Glutamate-mediated NMDA receptor stimulation leads to delayed activation of STEP via Ca^{2+}-dependent phosphatase calcineurin (Paul et al. 2003). The current study demonstrates that NR2B-NMDARs are responsible for the activation of STEP. This delayed activation of STEP, in turn, can limit

the activation of both p38 MAPK (current study) and ERK MAPK (Paul et al. 2003). Since prolonged activation of either ERK or p38 MAPK has been shown to be involved in neuronal apoptosis (Horstmann et al. 1998; Murray et al. 1998; Runden et al. 1998; Park et al. 2002; Stanciu and DeFranco 2002; Poddar and Paul 2009) these findings suggest a role of STEP in mediating the pro-survival effects of NMDA receptor stimulation.

It is not yet known why NR2A-containing NMDARs preferentially activate ERK and p38 MAPK, while STEP is more strongly activated by NR2B-containing receptors. However one possible mechanism involves differential Ca^{2+} dynamics triggered by these receptors. NMDA receptor mediated Ca^{2+} influx is required for activation of both MAPKs and STEP, and we have recently shown that NMDA receptor induced intracellular Ca^{2+} increases occur in two phases following exposure to high levels of glutamate. An initial rapid but small rise is followed by a gradual but larger increase. The delayed increase in Ca^{2+} is NR2B-NMDAR-dependent and strongly correlates with the delayed activation of STEP (Paul and Connor 2010). The two phase nature of the Ca^{2+} increase is also evident from electrophysiological studies in hippocampal neurons demonstrating that exposure to 100 μM NMDA leads to a rapidly developing inward current that would give rise to a rapid Ca^{2+} increase, followed by a larger slowly developing inward current that would give rise to a larger more slowly developing Ca^{2+} increase (Chen et al. 1997; Thompson et al. 2008). Taken together, it seems likely that a rapid initial Ca^{2+} increase (presumably due to NR2A-NMDA stimulation), is sufficient to activate ERK and p38 MAPK. Higher levels of Ca^{2+} influx via NR2B-NMDAR may initially activate cell survival pathways, including the activation of STEP. Consistent with this interpretation several previous studies in cultured neurons demonstrated that moderate increase in intracellular Ca^{2+} inhibits cell death induced by oxygen glucose deprivation and serum or growth factor withdrawal (Berridge et al. 2000; Chen et al. 2003; Cheng et al. 2003; Mottet et al. 2003; Bickler and Fahlman 2004). Moderate increase in Ca^{2+} also appears to be critical in the phenomenon of ischemic preconditioning in which tolerance to a severe ischemic insult is induced by antecedent of mild insult or stimulus (Grabb and Choi 1999; Semenov et al. 2002; Raval et al. 2003; Tauskela and Morley 2004). The extent to which Ca^{2+}-dependent STEP activation contributes to cell survival in these previous studies is not yet known. However this neuroprotection may become ineffective if the extracellular insult is sustained leading to accumulation of potentially lethal levels of Ca^{2+} and activation of detrimental pathways, which down-regulates the pro-survival factors that includes STEP.

A recent study showed that extrasynaptic NMDA receptor stimulation led to calpain-dependent cleavage of STEP, and proposed that this was an important contributor to excitotoxic neuronal injury (Xu et al. 2009). The results of our study are consistent with this general conclusion, as proteolytic cleavage of STEP was clearly observed following extended glutamate exposures, and maintaining STEP activity with the TAT-STEP peptide was sufficient to prevent neuronal injury. Furthermore, the TAT-STEP peptide also prevented *in vivo* injury strongly supporting the idea that targeting STEP breakdown could be an effective therapeutic approach.

Our results also reveal an important additional phase of p38 MAPK and STEP activation during glutamate-NMDA receptor stimulation that was not observed in the prior study. Immediately following glutamate treatment, a rapid initial activation of p38 MAPK is observed that is followed by a time-dependent decline due to the interaction of active STEP with p38 MAPK. Earlier studies have also reported activation of STEP following intracellular Ca^{2+} increase and activation of calcineurin (Paul et al. 2003; Snyder et al. 2005). It is difficult to explain why we saw this initial phase of p38 and STEP activation that was not observed in the study by Xu et al., (2009). One possibility is that the stimuli used in the present study (100 μM glutamate) permit more rapid activation of p38 and STEP,

compared with the approach of Xu et al., (2009) that used 10 μM NMDA along with bicuculline to stimulate extrasynaptic NMDARs.

Based on our data we suggest that irrespective of its anatomical location, NR2B-NMDAR stimulation can induce dephosphorylation and subsequent activation of STEP. Our hypothesis is that trans-synaptic stimulation of NR2B-NMDAR may lead to activation of STEP very close to the site of Ca^{2+} entry that plays a role in modulating synaptic plasticity through down regulation of ERK and p38 MAPK localized at the synaptic membrane. Whereas an excitotoxic insult leading to a more global increase in Ca^{2+} through all NR2B-NMDARs leads to overall increase in STEP activity that promotes neuroprotection by preventing the chronic activation and accumulation of p38 and ERK MAPK in the nucleus. However an extended insult may lead to STEP's degradation, facilitating cell death pathways.

The regulation of p38 MAPK activity by STEP described in the present study may also contribute to neuronal survival following stroke *in vivo*. A marked increase in extracellular glutamate levels has been observed in severe brain disorders such as ischemic stroke and traumatic brain injury and is responsible for NMDAR induced brain damage (Choi and Rothman 1990; Dirnagl et al. 1999). Activation of p38 MAPK has also been observed in the penumbral region following ischemic stroke (Barone et al. 2001a; Barone et al. 2001b; Cao et al. 2005; Nito et al. 2008) and plays a crucial role in ischemic brain injury. It is possible that degradation of active STEP is responsible for p38 MAPK activation in these models. Consistent with this hypothesis, a recent study using an animal model of ischemic stroke has shown that STEP is unilaterally down regulated in the stroked hemisphere over time. Furthermore, STEP levels are increased in a neuro-protective preconditioning paradigm, in regions of the brain that are resistant to ischemic brain damage (Braithwaite et al. 2008). p38 MAPK has been linked to an aberrant increase in expression of cyclooxgenase-2 (COX-2), an enzyme involved in the generation of pro-inflammatory prostanoids and reactive oxygen species (Rockwell et al. 2004; Moolwaney and Igwe 2005; Nito et al. 2008). Thus assessing the role of STEP in modulating COX-2 expression and pro-inflammatory responses may be helpful in determining whether the TAT-STEP peptide can be considered as a therapeutic agent to inhibit the progression of brain damage following ischemic stroke or related neurological disorders.

Supplementary Material

Refer to Web version on PubMed Central for supplementary material.

Acknowledgments

This work was supported by the National Institutes of Health grants NS059962 (Paul, S) and P20 RR015636 (Okada, Y). We would like to thank Dr. William Shuttleworth, University of New Mexico, for his helpful comments and Eduardo Estrada for technical assistance.

Abbreviations

MAPK	mitogen-activated protein kinase
APV	DL-2-amino-5-phosphonopentanoic acid,
CNQX	6-cyano-7-nitroquinoxaline-2,3-dione
STEP	striatal-enriched phosphatase
SDS	sodium dodecyl sulfate

PKA protein kinase A

References

Arundine M, Tymianski M. Molecular mechanisms of glutamate-dependent neurodegeneration in ischemia and traumatic brain injury. Cell Mol Life Sci 2004;61:657–668. [PubMed: 15052409]

Barone FC, Irving EA, Ray AM, Lee JC, Kassis S, Kumar S, Badger AM, Legos JJ, Erhardt JA, Ohlstein EH, Hunter AJ, Harrison DC, Philpott K, Smith BR, Adams JL, Parsons AA. Inhibition of p38 mitogen-activated protein kinase provides neuroprotection in cerebral focal ischemia. Medicinal research reviews 2001a;21:129–145. [PubMed: 11223862]

Barone FC, Irving EA, Ray AM, Lee JC, Kassis S, Kumar S, Badger AM, White RF, McVey MJ, Legos JJ, Erhardt JA, Nelson AH, Ohlstein EH, Hunter AJ, Ward K, Smith BR, Adams JL, Parsons AA. SB 239063, a second-generation p38 mitogen-activated protein kinase inhibitor, reduces brain injury and neurological deficits in cerebral focal ischemia. The Journal of pharmacology and experimental therapeutics 2001b;296:312–321. [PubMed: 11160612]

Berridge MJ, Lipp P, Bootman MD. The versatility and universality of calcium signalling. Nat Rev Mol Cell Biol 2000;1:11–21. [PubMed: 11413485]

Bickler PE, Fahlman CS. Moderate increases in intracellular calcium activate neuroprotective signals in hippocampal neurons. Neuroscience 2004;127:673–683. [PubMed: 15283966]

Bolshakov VY, Carboni L, Cobb MH, Siegelbaum SA, Belardetti F. Dual MAP kinase pathways mediate opposing forms of long-term plasticity at CA3-CA1 synapses. Nature neuroscience 2000;3:1107–1112.

Boulanger LM, Lombroso PJ, Raghunathan A, During MJ, Wahle P, Naegele JR. Cellular and molecular characterization of a brain-enriched protein tyrosine phosphatase. J Neurosci 1995;15:1532–1544. [PubMed: 7869116]

Braithwaite SP, Xu J, Leung J, Urfer R, Nikolich K, Oksenberg D, Lombroso PJ, Shamloo M. Expression and function of striatal enriched protein tyrosine phosphatase is profoundly altered in cerebral ischemia. The European journal of neuroscience 2008;27:2444–2452. [PubMed: 18445231]

Bult A, Zhao F, Dirkx R Jr, Raghunathan A, Solimena M, Lombroso PJ. STEP: a family of brain-enriched PTPs. Alternative splicing produces transmembrane, cytosolic and truncated isoforms. European journal of cell biology 1997;72:337–344. [PubMed: 9127733]

Cao J, Viholainen JI, Dart C, Warwick HK, Leyland ML, Courtney MJ. The PSD95-nNOS interface: a target for inhibition of excitotoxic p38 stress-activated protein kinase activation and cell death. The Journal of cell biology 2005;168:117–126. [PubMed: 15631993]

Chen QX, Perkins KL, Choi DW, Wong RK. Secondary activation of a cation conductance is responsible for NMDA toxicity in acutely isolated hippocampal neurons. J Neurosci 1997;17:4032–4036. [PubMed: 9151719]

Chen WG, Chang Q, Lin Y, Meissner A, West AE, Griffith EC, Jaenisch R, Greenberg ME. Derepression of BDNF transcription involves calcium-dependent phosphorylation of MeCP2. Science (New York, N Y 2003;302:885–889.

Cheng A, Wang S, Yang D, Xiao R, Mattson MP. Calmodulin mediates brain-derived neurotrophic factor cell survival signaling upstream of Akt kinase in embryonic neocortical neurons. The Journal of biological chemistry 2003;278:7591–7599. [PubMed: 12488453]

Choi DW, Rothman SM. The role of glutamate neurotoxicity in hypoxic-ischemic neuronal death. Annual review of neuroscience 1990;13:171–182.

Dirnagl U, Iadecola C, Moskowitz MA. Pathobiology of ischaemic stroke: an integrated view. Trends in neurosciences 1999;22:391–397. [PubMed: 10441299]

Gisabella B, Rowan MJ, Anwyl R. Mechanisms underlying the inhibition of long-term potentiation by preconditioning stimulation in the hippocampus in vitro. Neuroscience 2003;121:297–305. [PubMed: 14521989]

Grabb MC, Choi DW. Ischemic tolerance in murine cortical cell culture: critical role for NMDA receptors. J Neurosci 1999;19:1657–1662. [PubMed: 10024352]

Haelewyn B, Alix P, Maubert E, Abraini JH. NMDA-induced striatal brain damage and time-dependence reliability of thionin staining in rats. Journal of neuroscience methods 2008;168:479–482. [PubMed: 18063092]

Horstmann S, Kahle PJ, Borasio GD. Inhibitors of p38 mitogen-activated protein kinase promote neuronal survival in vitro. Journal of neuroscience research 1998;52:483–490. [PubMed: 9589393]

Iadecola C, Niwa K, Nogawa S, Zhao X, Nagayama M, Araki E, Morham S, Ross ME. Reduced susceptibility to ischemic brain injury and N-methyl-D-aspartate-mediated neurotoxicity in cyclooxygenase-2-deficient mice. Proceedings of the National Academy of Sciences of the United States of America 2001;98:1294–1299. [PubMed: 11158633]

Ingram AJ, James L, Thai K, Ly H, Cai L, Scholey JW. Nitric oxide modulates mechanical strain-induced activation of p38 MAPK in mesangial cells. Am J Physiol Renal Physiol 2000;279:F243–251. [PubMed: 10919842]

Kawasaki H, Morooka T, Shimohama S, Kimura J, Hirano T, Gotoh Y, Nishida E. Activation and involvement of p38 mitogen-activated protein kinase in glutamate-induced apoptosis in rat cerebellar granule cells. The Journal of biological chemistry 1997;272:18518–18521. [PubMed: 9228012]

Kim MJ, Dunah AW, Wang YT, Sheng M. Differential roles of NR2A-and NR2B-containing NMDA receptors in Ras-ERK signaling and AMPA receptor trafficking. Neuron 2005;46:745–760. [PubMed: 15924861]

Kohr G. NMDA receptor function: subunit composition versus spatial distribution. Cell and tissue research 2006;326:439–446. [PubMed: 16862427]

Kumar S, Boehm J, Lee JC. p38 MAP kinases: key signalling molecules as therapeutic targets for inflammatory diseases. Nat Rev Drug Discov 2003;2:717–726. [PubMed: 12951578]

Lipton SA, Rosenberg PA. Excitatory amino acids as a final common pathway for neurologic disorders. The New England journal of medicine 1994;330:613–622. [PubMed: 7905600]

Liu Y, Wong TP, Aarts M, Rooyakkers A, Liu L, Lai TW, Wu DC, Lu J, Tymianski M, Craig AM, Wang YT. NMDA receptor subunits have differential roles in mediating excitotoxic neuronal death both in vitro and in vivo. J Neurosci 2007;27:2846–2857. [PubMed: 17360906]

Luo J, Wang Y, Yasuda RP, Dunah AW, Wolfe BB. The majority of N-methyl-D-aspartate receptor complexes in adult rat cerebral cortex contain at least three different subunits (NR1/NR2A/NR2B). Molecular pharmacology 1997;51:79–86. [PubMed: 9016349]

Moolwaney AS, Igwe OJ. Regulation of the cyclooxygenase-2 system by interleukin-1beta through mitogen-activated protein kinase signaling pathways: a comparative study of human neuroglioma and neuroblastoma cells. Brain Res Mol Brain Res 2005;137:202–212. [PubMed: 15950779]

Mottet D, Michel G, Renard P, Ninane N, Raes M, Michiels C. Role of ERK and calcium in the hypoxia-induced activation of HIF-1. Journal of cellular physiology 2003;194:30–44. [PubMed: 12447987]

Mukherjee PK, DeCoster MA, Campbell FZ, Davis RJ, Bazan NG. Glutamate receptor signaling interplay modulates stress-sensitive mitogen-activated protein kinases and neuronal cell death. The Journal of biological chemistry 1999;274:6493–6498. [PubMed: 10037742]

Murray B, Alessandrini A, Cole AJ, Yee AG, Furshpan EJ. Inhibition of the p44/42 MAP kinase pathway protects hippocampal neurons in a cell-culture model of seizure activity. Proceedings of the National Academy of Sciences of the United States of America 1998;95:11975–11980. [PubMed: 9751775]

Nguyen TH, Liu J, Lombroso PJ. Striatal enriched phosphatase 61 dephosphorylates Fyn at phosphotyrosine 420. The Journal of biological chemistry 2002;277:24274–24279. [PubMed: 11983687]

Nito C, Kamada H, Endo H, Niizuma K, Myer DJ, Chan PH. Role of the p38 mitogen-activated protein kinase/cytosolic phospholipase A2 signaling pathway in blood-brain barrier disruption after focal cerebral ischemia and reperfusion. J Cereb Blood Flow Metab 2008;28:1686–1696. [PubMed: 18545259]

Park JG, Yuk Y, Rhim H, Yi SY, Yoo YS. Role of p38 MAPK in the regulation of apoptosis signaling induced by TNF-alpha in differentiated PC12 cells. Journal of biochemistry and molecular biology 2002;35:267–272. [PubMed: 12297009]

Paul S, Connor J. NR2B-NMDA receptor mediated increases in intracellular Ca2+ concentration regulate the tyrosine phosphatase, STEP, and ERK MAP kinase signaling. Journal of neurochemistry. 2010 In Press.

Paul S, Nairn AC, Wang P, Lombroso PJ. NMDA-mediated activation of the tyrosine phosphatase STEP regulates the duration of ERK signaling. Nature neuroscience 2003;6:34–42.

Paul S, Snyder GL, Yokakura H, Picciotto MR, Nairn AC, Lombroso PJ. The Dopamine/D1 receptor mediates the phosphorylation and inactivation of the protein tyrosine phosphatase STEP via a PKA-dependent pathway. J Neurosci 2000;20:5630–5638. [PubMed: 10908600]

Paul S, Olausson P, Venkitaramani DV, Ruchkina I, Moran TD, Tronson N, Mills E, Hakim S, Salter MW, Taylor JR, Lombroso PJ. The striatal-enriched protein tyrosine phosphatase gates long-term potentiation and fear memory in the lateral amygdala. Biological psychiatry 2007;61:1049–1061. [PubMed: 17081505]

Paxinos, G.; Watson, C. The Rat Brain in Stereotaxic Coordinates. New York: Academic Press; 1986.

Poddar R, Paul S. Homocysteine-NMDA receptor-mediated activation of extracellular signal-regulated kinase leads to neuronal cell death. Journal of neurochemistry 2009;110:1095–1106. [PubMed: 19508427]

Pulido R, Zuniga A, Ullrich A. PTP-SL and STEP protein tyrosine phosphatases regulate the activation of the extracellular signal-regulated kinases ERK1 and ERK2 by association through a kinase interaction motif. The EMBO journal 1998;17:7337–7350. [PubMed: 9857190]

Raval AP, Dave KR, Mochly-Rosen D, Sick TJ, Perez-Pinzon MA. Epsilon PKC is required for the induction of tolerance by ischemic and NMDA-mediated preconditioning in the organotypic hippocampal slice. J Neurosci 2003;23:384–391. [PubMed: 12533598]

Rockwell P, Martinez J, Papa L, Gomes E. Redox regulates COX-2 upregulation and cell death in the neuronal response to cadmium. Cellular signalling 2004;16:343–353. [PubMed: 14687664]

Rodrigues SM, Schafe GE, LeDoux JE. Intra-amygdala blockade of the NR2B subunit of the NMDA receptor disrupts the acquisition but not the expression of fear conditioning. J Neurosci 2001;21:6889–6896. [PubMed: 11517276]

Runden E, Seglen PO, Haug FM, Ottersen OP, Wieloch T, Shamloo M, Laake JH. Regional selective neuronal degeneration after protein phosphatase inhibition in hippocampal slice cultures: evidence for a MAP kinase-dependent mechanism. J Neurosci 1998;18:7296–7305. [PubMed: 9736650]

Semenov DG, Samoilov MO, Lazarewicz JW. Calcium transients in the model of rapidly induced anoxic tolerance in rat cortical slices: involvement of NMDA receptors. Neuro-Signals 2002;11:329–335. [PubMed: 12566922]

Snyder EM, Nong Y, Almeida CG, Paul S, Moran T, Choi EY, Nairn AC, Salter MW, Lombroso PJ, Gouras GK, Greengard P. Regulation of NMDA receptor trafficking by amyloid-beta. Nature neuroscience 2005;8:1051–1058.

Stanciu M, DeFranco DB. Prolonged nuclear retention of activated extracellular signal-regulated protein kinase promotes cell death generated by oxidative toxicity or proteasome inhibition in a neuronal cell line. The Journal of biological chemistry 2002;277:4010–4017. [PubMed: 11726647]

Tauskela JS, Morley P. On the role of Ca2+ in cerebral ischemic preconditioning. Cell calcium 2004;36:313–322. [PubMed: 15261487]

Thomas GM, Huganir RL. MAPK cascade signalling and synaptic plasticity. Nature reviews 2004;5:173–183.

Thompson RJ, Jackson MF, Olah ME, Rungta RL, Hines DJ, Beazely MA, MacDonald JF, MacVicar BA. Activation of pannexin-1 hemichannels augments aberrant bursting in the hippocampus. Science (New York, N Y 2008;322:1555–1559.

Tovar KR, Westbrook GL. The incorporation of NMDA receptors with a distinct subunit composition at nascent hippocampal synapses in vitro. J Neurosci 1999;19:4180–4188. [PubMed: 10234045]

Tu W, Xu X, Peng L, Zhong X, Zhang W, Soundarapandian MM, Balel C, Wang M, Jia N, Zhang W, Lew F, Chan SL, Chen Y, Lu Y. DAPK1 interaction with NMDA receptor NR2B subunits mediates brain damage in stroke. Cell 2010;140:222–234. [PubMed: 20141836]

Walker DL, Davis M. Amygdala infusions of an NR2B-selective or an NR2A-preferring NMDA receptor antagonist differentially influence fear conditioning and expression in the fear-potentiated startle test. Learning & memory (Cold Spring Harbor, N Y 2008;15:67–74.

Wang Q, Walsh DM, Rowan MJ, Selkoe DJ, Anwyl R. Block of long-term potentiation by naturally secreted and synthetic amyloid beta-peptide in hippocampal slices is mediated via activation of the kinases c-Jun N-terminal kinase, cyclin-dependent kinase 5, and p38 mitogen-activated protein kinase as well as metabotropic glutamate receptor type 5. J Neurosci 2004;24:3370–3378. [PubMed: 15056716]

Waxman EA, Lynch DR. N-methyl-D-aspartate receptor subtype mediated bidirectional control of p38 mitogen-activated protein kinase. The Journal of biological chemistry 2005;280:29322–29333. [PubMed: 15967799]

Xu J, Kurup P, Zhang Y, Goebel-Goody SM, Wu PH, Hawasli AH, Baum ML, Bibb JA, Lombroso PJ. Extrasynaptic NMDA receptors couple preferentially to excitotoxicity via calpain-mediated cleavage of STEP. J Neurosci 2009;29:9330–9343. [PubMed: 19625523]

Zhao MG, Toyoda H, Lee YS, Wu LJ, Ko SW, Zhang XH, Jia Y, Shum F, Xu H, Li BM, Kaang BK, Zhuo M. Roles of NMDA NR2B subtype receptor in prefrontal long-term potentiation and contextual fear memory. Neuron 2005;47:859–872. [PubMed: 16157280]

Zhu JJ, Qin Y, Zhao M, Van Aelst L, Malinow R. Ras and Rap control AMPA receptor trafficking during synaptic plasticity. Cell 2002;110:443–455. [PubMed: 12202034]

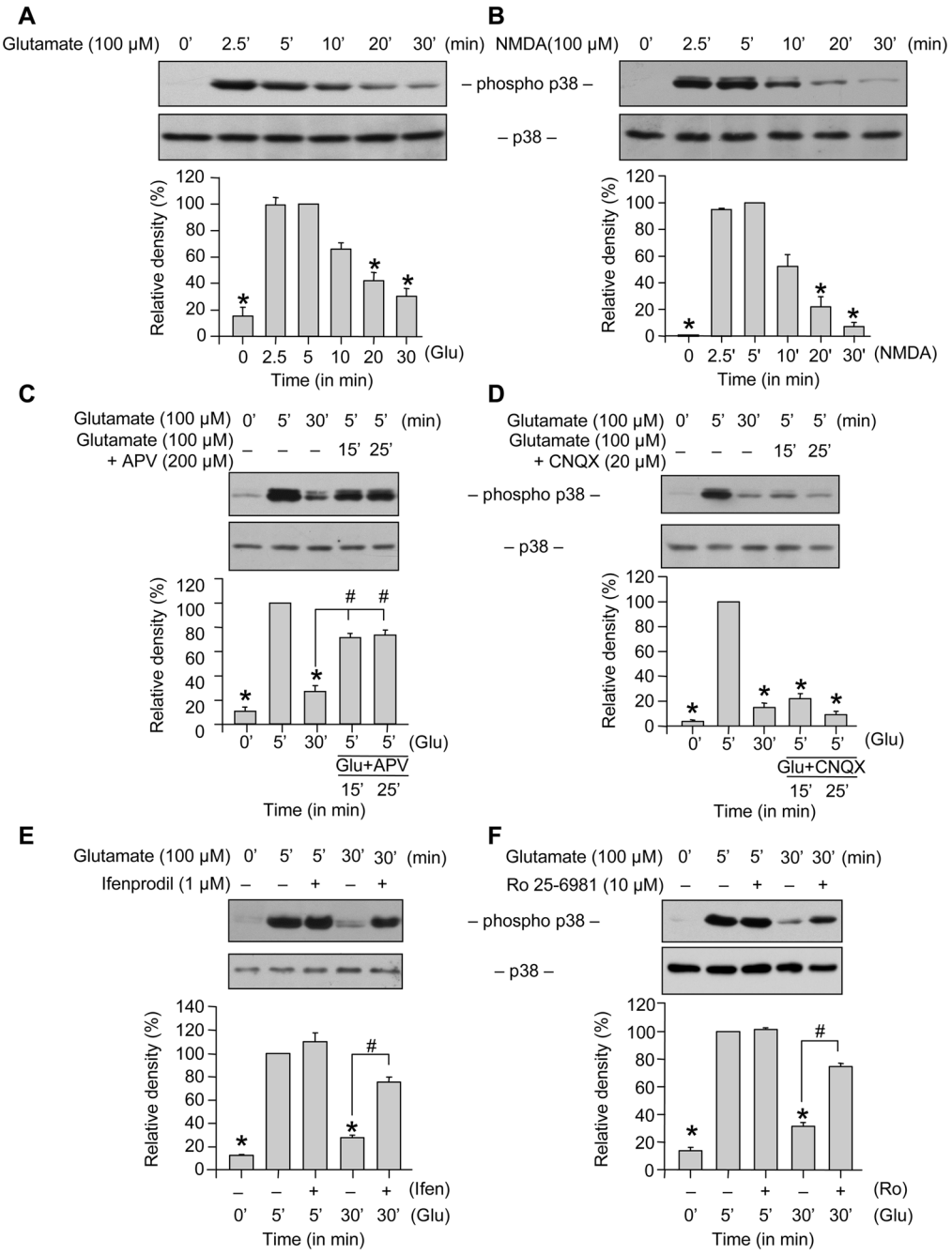

Figure 1.

Role of NR2B-NMDARs in glutamate-NMDAR induced transient phosphorylation of p38 MAPK. Neuron cultures were treated with (A) glutamate (100 μM) or (B) NMDA (100 μM) for the specified times. (C-D) Neurons were treated with glutamate for the specified times. For lanes 4 and 5, after treatment with glutamate for 5 min, APV (C) or CNQX (D) was added and the incubation was continued for the specified times. (E, F) Neurons were treated with 100 μM glutamate for specified times in the presence or absence of ifenprodil (E) or Ro 25-6981 (F). Equal amount of protein from each sample was processed for immunoblot analysis using anti-phospho p38 ($T^{P}EY^{P}$-p38, upper panel) and p38 (lower panel) antibodies. Quantification of phosphorylated p38 MAPK by computer-assisted densitometry

and Image J analysis is shown below each immunoblot. Values are mean ± SEM (n ≥ 3). *Indicates significant difference from 5 min glutamate or NMDA treatment ($p < 0.001$). #Indicates significant difference from 30 min glutamate treatment ($p < 0.001$).

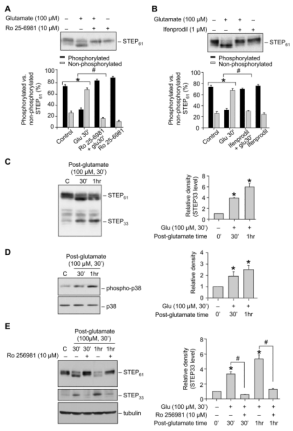

Figure 2.

Glutamate/NMDAR induced dephosphorylation and subsequent cleavage of STEP involves NR2B-NMDARs. Neuronal cultures were treated with (A-B) 100 μM glutamate for 30 min in the presence or absence of Ro 25-6981 (A) or ifenprodil (B); (C-D) 100 μM glutamate for 30 min and maintained in its original medium for the specified times (post-glutamate time); (E) 100 μM glutamate for 30 min in the presence or absence of Ro 25-6981 and maintained in its original medium for the specified time (post-glutamate time). Extracts with equal amount of protein were analyzed from each sample with anti-STEP antibody (A, B, C; upper and middle panel of E). In some samples phosphorylation of p38 was analyzed using anti-phospho p38 antibody ($T^{P}EY^{P}$-p38; upper panel, D). Total p38 or tubulin was analyzed by re-probing the membrane with either anti-p38 (lower panel, D) or anti-tubulin antibody (lower panel, E). Quantification of (A-B) phosphorylated (upper band) and non-phosphorylated (lower band) STEP was done using computer assisted densitometry and Image J analysis and data presented as percentage of the total; (C, E) extent of proteolytic cleavage of STEP and (D) phosphorylation of p38 MAPK was done using computer assisted densitometry and Image J analysis. Values are mean ± SEM (n ≥ 3). *Indicates significant difference from control ($p < 0.001$). #Indicates significant difference from 30 min or 1 hr glutamate treatment ($p < 0.001$).

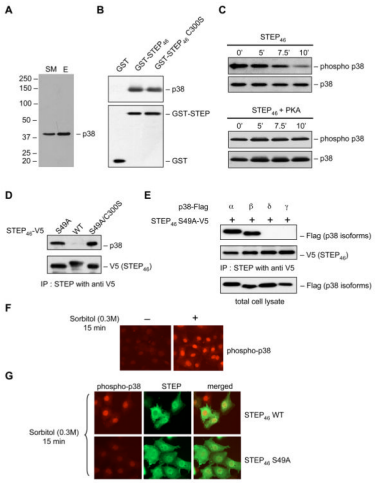

Figure 3.

p38 MAPK is a substrate of STEP. (A) Rat brain homogenates were passed through $STEP_{46}$ C300S affinity column. Eluants were processed for immunoblot analysis using anti-p38 MAPK antibody (SM- starting material, E- eluant). (B) GST, GST-$STEP_{46}$ or GST-$STEP_{46}$ C300S fusion proteins were incubated with recombinant p38 MAPK protein. Bound proteins were extracted and processed for immunoblot analysis using anti-p38 MAPK (upper panel) antibody. Blots were re-probed with anti-GST (lower panel) antibody. (C) GST-$STEP_{46}$ or GST-$STEP_{46}$ phosphorylated with PKA were incubated with active p38α MAPK (phosphorylated at the regulatory threonine and tyrosine residues) for the specified times. Samples were analyzed using a phospho-specific antibody that recognizes p38 MAPK when it is phosphorylated at the regulatory tyrosine residue (TEY^P-p38). Blots were re-probed with anti-p38 MAPK antibody. (D-E) Hela cells were transfected with (D) V5-$STEP_{46}$ or one of its mutants (S49A and S49A/C300S); or (E) V5-$STEP_{46}$ S49A and Flag-tagged p38α, β, γ or δ. STEP was immunoprecipitated with anti-V5 antibody. Samples were analyzed either with anti-p38 (upper panel, D) or -anti Flag antibody (upper panel, E). Blots were re-probed with anti-V5-HRP antibody (lower panel, D-E). In E total lysate was analyzed using anti-Flag antibody to demonstrate expression of all p38 isoforms in Hela cells. (F-G) Untransfected Hela cells (F) and Hela cell transfected with V5-$STEP_{46}$ or V5-$STEP_{46}$-S49A (G) were treated with 0.3M sorbitol for 15 min and processed for immunocytochemical staining with anti-phospho p38 (T^PEY^P-p38; F, G) and anti-V5-HRP (G) antibodies.

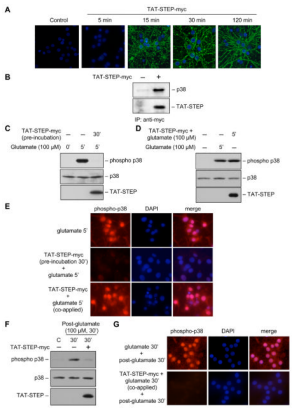

Figure 4.

TAT-STEP-myc peptide can block phosphorylation and nuclear translocation of p38 MAPK. (A) Neuronal cultures were incubated with the TAT-STEP-myc peptide for the specified times and processed for immunocytochemical staining with anti-myc antibody. (B) Neuronal cultures were incubated with TAT-STEP-myc peptide (30 min) followed by immunoprecipitation with anti-myc antibody. Samples were analyzed using anti phospho-p38 antibody (T^PEY^P-p38, upper panel). Blots were re-probed with anti-myc antibody (lower panel). (C-E) Neuronal cultures were treated with glutamate (100 μM, 5 min) in the absence or presence of TAT-STEP-myc peptide. The peptide was applied to neurons either 30 min prior to (C, E: middle panel) or along with glutamate (D, E: lower panel). (C-D) Cell lysates were analyzed using anti-phospho-p38 antibody (T^PEY^P-p38, upper panel), Blots were re-probed with anti-p38 (C, D: middle panel) or anti-myc (C, D: lower panel) antibodies. (E) Cells were processed for immunocytochemical analysis with anti-phospho p38 antibody (T^PEY^P-p38) and DAPI. (F-G) Neuron cultures were treated with glutamate (100 μM, 30 min) in the absence or presence of TAT-STEP-myc peptide. The peptide was co-applied along with glutamate. 30 min after termination of glutamate treatment cells were processed either for (F) immunoblot analysis using anti-phospho-p38 (T^PEY^P-p38, upper panel), -p38 (middle panel) and -myc (lower panel) antibodies respectively or (G) for immunocytochemical analysis with anti-phospho p38 antibody (T^PEY^P-p38) and DAPI.

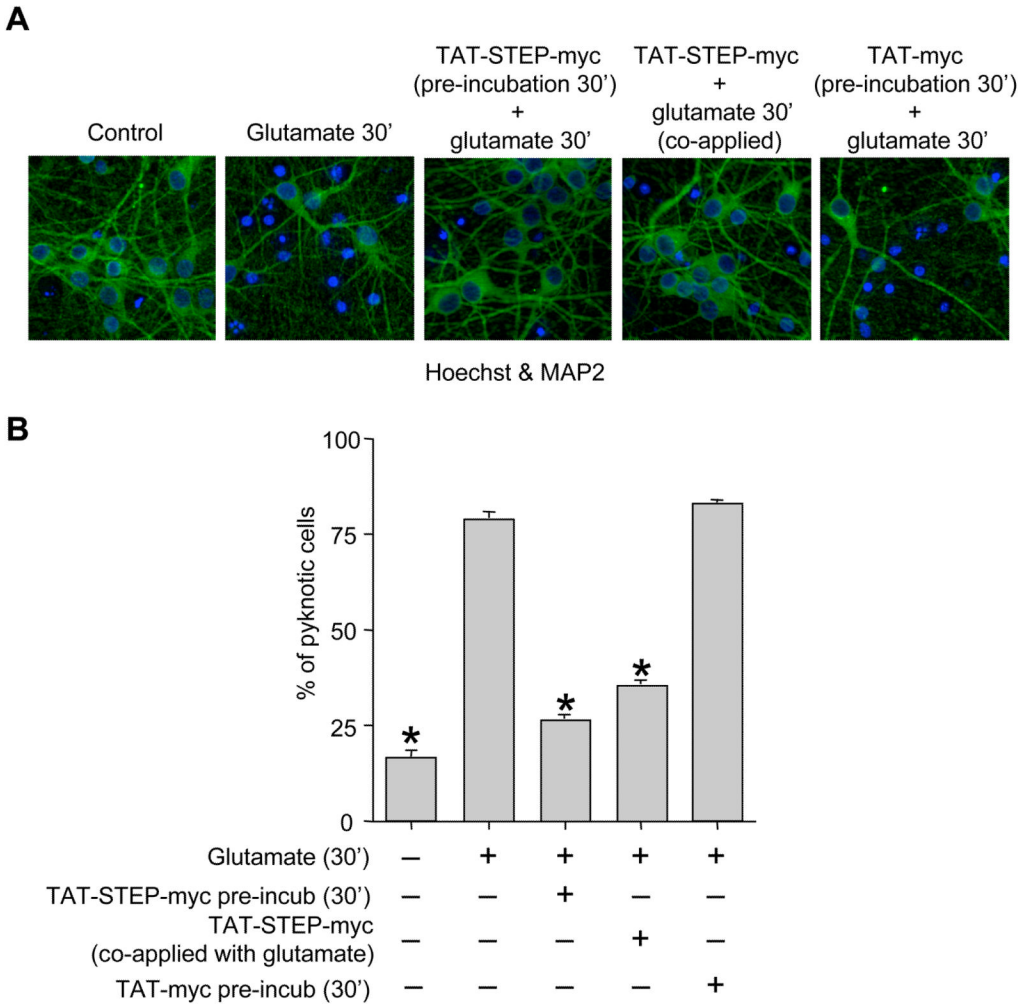

Figure 5.

TAT-STEP-myc peptide reduces glutamate-induced neuronal cell death. Neuronal cultures were treated with glutamate (100 μM, 30 min) in the absence or presence of TAT-STEP-myc peptide or the corresponding TAT-myc control and then maintained in the original medium for another 20 hr. TAT-STEP-myc peptide was applied to cells either 30 min prior to or along with glutamate. (A) Representative photomicrograph demonstrating the extent of cell death, by immunocytochemical analysis with anti-MAP2 antibody and Hoechst DNA staining. (B) Quantitative analysis of the percentage of neurons with pyknotic nuclei is represented as mean ± SEM ($n \geq 3$). *Indicates significant difference from 30 min glutamate treatment ($p < 0.001$).

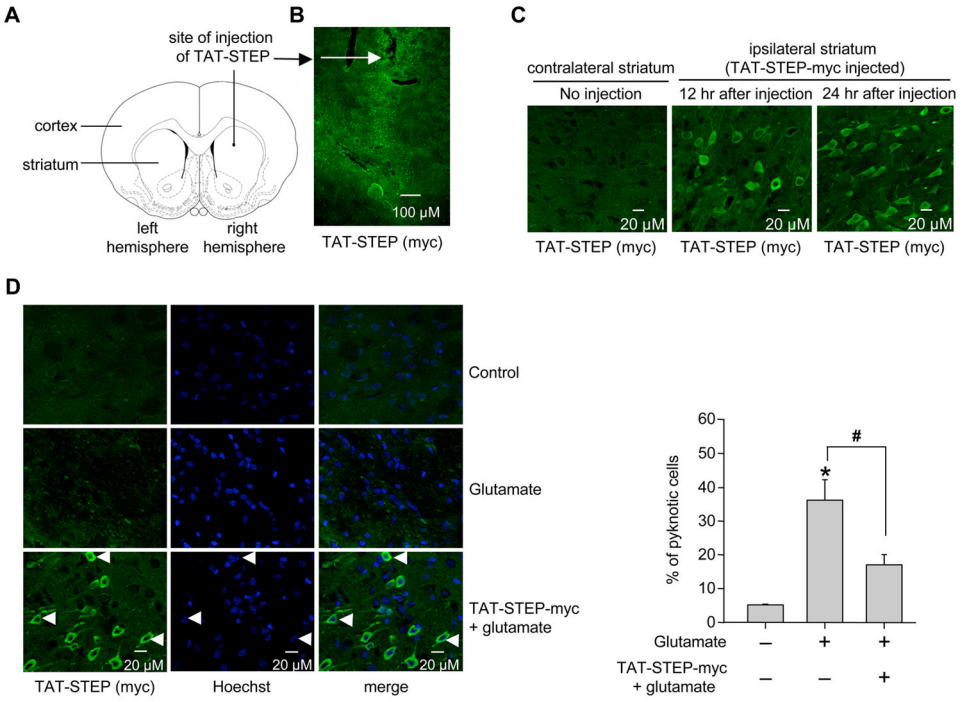

Figure 6.

TAT-STEP-myc peptide reduces glutamate-induced cell death in the striatum. (A) Schematic representation of the area of infusion of TAT-STEP-myc peptide. (B-C) TAT-STEP-myc peptide was stereotactically injected into the striatum. Coronal sections were processed for immunohistochemical analysis with anti-myc antibody at the specified time periods. (B) Low magnification (5X) and (C) high magnification (20X) images. (D) Glutamate was injected stereotactically into the striatum in the presence or absence of TAT-STEP-myc peptide. Striatal brain sections were processed for immunohistochemical analysis with anti-myc antibody and Hoechst DNA stain (left panel). Quantitative analysis of the percentage of neurons with pyknotic nuclei is represented as mean ± SEM ($n \geq 3$, right panel). *Indicates significant difference from glutamate treated samples ($p < 0.001$).